doi:10.1038/nature14327

Supplementary Text

Structure solution and Rietveld refinement of mmen-Mn_2(dobpdc)

Initially, the previously reported crystal structure of the isostructural Zn_2(dobpdc)[13], with the Zn atoms replaced by Mn atoms, was used to calculate a Fourier difference map for mmen-Mn_2(dobpdc). While the Fourier difference maps revealed excess electron density above each Mn site as expected (Extended Data Figure 1e), it was not possible to definitively locate the individual atoms of the appended mmen groups using standard Fourier difference methods. This is a common occurrence when solving crystal structures from powder diffraction data and is primarily due to the significant overlap of intensity from Bragg reflections that occur at nearly, and often exactly, identical diffraction angles. As a result, direct space methods are often necessary to develop a structural model that can be used for Rietveld refinement. This is particularly true when a large number of atoms need to be found, as is the case for both mmen-Mn_2(dobpdc) and CO_2-mmen-Mn_2(dobpdc).

Here, the structure solution of mmen-Mn_2(dobpdc) at 100 K was performed in direct space using the simulated annealing technique, as implemented in TOPAS-Academic. During the simulated annealing process, a rigid, idealized model was employed for the full mmen ligand and for the crystallographically independent portion of the dopbdc^{4-} moiety (one-half ligand). For the mmen rigid body, three dihedral angles were randomized during simulated annealing. In order to arrive at a chemically reasonable structural model for mmen-Mn_2(dobpdc), additional structural information, including distance restraints and "anti-bump" penalties, were incorporated into the simulated annealing search for a global minimum.

Once an initial structural model was developed, a complete refinement was preformed using the Rietveld method, maintaining the rigid bodies for mmen and dobpdc^{4-} during the refinement process. Note that, in contrast to the CO_2-mmen-Mn_2(dobpdc) compound, the diffraction data was not of sufficient quality at high angles to allow for the independent refinement of all atomic positions. Instead, the three dihedral angles of mmen (dih 1-3) were fully refined, as was the position (x, y, z) and orientation (α, β, γ) of the mmen and dobpdc^{4-} rigid bodies. Additionally, the rotation angle of the carboxylate (rot 1) and all C−C bond distances in the dobpdc^{4-} rigid body were fully refined, as was the Mn atomic position.

A single refined isotropic thermal parameter was assigned to the Mn atom and was free to vary. A single isotropic thermal parameter was assigned to all atoms of the dobpdc^{4-} ligand and was refined with no constraints. With the exception of the metal-bound N atom of mmen (N1m), a single isotropic thermal parameter was assigned to all other mmen atoms, which was refined with no constraints. Note that the fractional occupancies of each mmen atom were constrained to be the same, and the total mmen occupancy was refined. During the initial stages of the Rietveld refinement, excess electron density was observed near the metal-bound N atom of mmen (N1m) and was located at a distance typical of an N−C single bond. This excess electron density was attributed to disorder of the CH_3 bound to N1m since N1m becomes a stereocenter after binding to Mn. This disorder was subsequently modeled with the CH_3 group bound to N1m being disordered over two sites C1ma and C1mb. The total occupancy of the disordered CH_3 groups was constrained to be equal to the total mmen occupancy, but the relative occupancies of each site were free to vary. Finally, all H atoms were constrained to follow the C and N atoms they

were bound to, and their atomic positions were not refined independently. The calculated diffraction pattern for the final structural model of mmen-Mn_2(dobpdc) is in excellent agreement with the experimental diffraction pattern (Extended Data Figure 1a).

Structure solution and Rietveld refinement of CO_2-mmen-Mn_2(dobpdc)

After dosing with CO_2, significant changes in the relative intensities of Bragg diffraction peaks were observed, indicating a structural transition upon CO_2 adsorption (Extended Data Figure 1d). In a manner similar to that described for mmen-Mn_2(dobpdc), the structure solution of CO_2-mmen-Mn_2(dobpdc) at 100 K was performed in direct space using the simulated annealing technique, as implemented in TOPAS-Academic. Based on the IR and solid-state NMR results described earlier, there was strong evidence for the formation of ammonium carbamate upon CO_2 adsorption. As such, a rigid, idealized model was developed for the ammonium carbamate moiety, which was based on the reported single crystal structure of methyl(2-(methylammonio)ethyl)-carbamate.[21] During the simulated annealing process, four dihedral angles of the ammonium carbamate were randomized. In order to arrive at a chemically reasonable structural model for CO_2-mmen-Mn_2(dobpdc), additional structural information, including distance restraints and "anti-bump" penalties, were incorporated into the simulated annealing search for a global minimum.

Once an initial structural model was developed, a complete refinement was preformed using the Rietveld method, maintaining the rigid bodies at the initial stages but independently refining all atomic positions in the final cycles of refinement. Note that while the high quality of the diffraction data allowed all atomic positions to be independently refined, a small number of weak C−C and C−N distance restraints were maintained for the purpose of keeping C−C and C−N bond distances within a chemically reasonable range so as to avoid fitting noise in the diffraction data. With the exception of the dobpdc^{4-} atoms, an independent isotropic thermal parameter was assigned to each C, N, O, and Mn atom, and these parameters were free to vary. A single isotropic thermal parameter was assigned to all atoms of the dobpdc^{4-} ligand and was refined with no constraints. Note that the fractional occupancies of each ammonium carbamate atom were constrained to be the same, and the total occupancy was refined freely. Finally, H atoms were constrained to follow the C and N atoms they were bound to, and their atomic positions were not refined independently.

Note that we did not observe any disorder during the refinement process. However, the thermal parameter of the ammonium N atom (N2m) was observed to increase significantly during the refinement. This larger thermal parameter is likely accounting for either thermal motion of the ammonium or a small amount of disorder in the ammonium site position. Since the ammonium has several relatively close interactions with the framework and neighboring carbamate, some disorder or thermal motion might be expected; but regardless, the ESDs of the calculated bond distances are not significantly affected by the large thermal parameter. Additionally, all attempts at modeling any potential disorder with multiple site positions did not improve the overall quality of the refinement, and we opted to capture any disorder by allowing all thermal parameters to vary freely. Most importantly, the calculated diffraction pattern for the final structural model of CO_2-mmen-Mn_2(dobpdc) is in excellent agreement with the experimental diffraction pattern (Extended Data Figure 1 b).

A full Rietveld refinement was similarly performed against the diffraction data collected for CO_2-mmen-Mn_2(dobpdc) at 295 K. Initially, the 100 K structural model was used for the refinement, and the calculated diffraction intensities showed excellent agreement with the experimental. Here, a single isotropic thermal parameter was assigned to all atoms of the dobpdc^{4-} ligand and was refined with no constraints. With the exception of the metal-bound O atom of the carbamate (O1m), a single isotropic thermal parameter was assigned to all atoms of the ammonium carbamate and was free to vary. Note that, as expected, all refined thermal parameters increased moderately compared to the 100 K structure. The refined ammonium carbamate occupancy is slightly higher for the 295 K structure than the 100 K structure due to the higher partial pressure of CO_2 (100 mbar) that was dosed for the 295 K sample (compared to 5 mbar for the 100 K sample). The calculated diffraction pattern for the final structural model of CO_2-mmen-Mn_2(dobpdc) is in excellent agreement with the experimental diffraction pattern, demonstrating that the well-ordered ammonium-carbamate chain structure is maintained at 295 K (Extended Data Figure 1c).

Isotherm fitting and isosteric heats of adsorption

In order to calculate isosteric heats of adsorption, Q_{st}, as a function of the amount of CO_2 adsorbed, the temperature-dependent adsorption data for each mmen-M_2(dobpdc) compound was fit with a mathematical model. Since mmen-Ni_2(dobpdc) does not have any isotherm steps in the adsorption data measured for this work, the isotherm data was fit with a classical dual-site Langmuir-Freundlich equation. Owing to the sharp step in many of the CO_2 adsorption isotherms, fitting with a continuous function was not possible, and a piecewise function (Eqn 1) was developed to describe both the pre-step and post-step CO_2 adsorption for all other compounds at each temperature. Specifically, when the pressure, p, is less than the step pressure, p_{step}, at a given temperature, T, the isotherm is modeled using a classical single-site Langmuir-Freundlich equation where R is the ideal gas constant in J mol^{-1} K^{-1}, n_{sat} is the saturation capacity in mmol/g, S is the integral entropy of adsorption at saturation in units of R, H is the differential enthalpy of adsorption in kJ/mol, and v is the Freundlich parameter. When the p is greater than p_{step}, the isotherm is modeled using a dual-site Langmuir-Freundlich equation, with two adsorption sites a and b, for which p has been offset by p_{step}. The temperature dependence of p_{step} is described using the Clausius-Clapeyron relation (Eqn 2), as is standard for evaluating the temperature dependence of any phase transition. Here, p_{step} is a function of the step pressure at an initial temperature, $P_{step,T0}$, and the enthalpy of the phase transition that is associated with the step, H_{step}. The stepped CO_2 adsorption isotherms for at least 3 temperatures are fit simultaneously with one set of parameters for each mmen-M_2(dobpdc) compound. The resulting calculated CO_2 adsorption isotherms agree well with the experimental data (Fig. S7). We note that there is a slight discontinuity when p is just above p_{step} and n is less than $n(p_{step})$, but this does not affect the isosteric heat of adsorption calculations.

$$n(P,T)=\begin{cases}\dfrac{n_{sat,1}e^{S_1}e^{-H_1/RT}p^{v_1}}{1+e^{S_1}e^{-H_1/RT}p^{v_1}} & \text{if } p \le p_{step} \\ \dfrac{n_{sat,2a}e^{S_{2a}}e^{-H_{step}/RT}\left(p-p_{step}\right)^{v_{2a}}}{1+e^{S_{2a}}e^{-H_{step}/RT}\left(p-p_{step}\right)^{v_{2a}}}+\dfrac{n_{sat,2b}e^{S_{2b}}e^{-H_{2b}/RT}\left(p-p_{step}\right)^{v_{2b}}}{1+e^{S_{2b}}e^{-H_{2b}/RT}\left(p-p_{step}\right)^{v_{2b}}} & \text{if } p > p_{step}\end{cases} \quad (1)$$

$$p_{\text{step}}(T) = p_{\text{step},T_0} e^{\left(\frac{H_{\text{step}}}{R}\right)\left(\frac{1}{T_o}-\frac{1}{T}\right)} \quad (2)$$

The isosteric heats of adsorption can be calculated by solving Eqn 1 for explicit values of n at a minimum of 3 temperatures. The isosteric heats of adsorption as a function of the amount of CO_2 adsorbed can then be determined using the integrated form of the Clausius-Clapeyron equation (Eqn 3) by calculating the slope of ln(p) vs 1/T for each loading.

$$(\ln p)_n = \left(\frac{Q_{\text{st}}}{R}\right)\left(\frac{1}{T}\right) + C \quad (3)$$

Regeneration energy calculations

Regeneration energy values were calculated from estimations of the latent and sensible heat contributions per kg of CO_2 captured for a pure temperature swing adsorption process (no vacuum or inert gas purge). Latent heat contributions were derived from the aforementioned calculated isosteric heats of adsorptions. Sensible heat contributions were determined using average heat capacities. Owing to the expected gradual increase in heat capacities versus temperature, the heat capacity of mmen-Mg_2(dobpdc) (1.6 J/g·K) was determined from the heat flow into the sample as it was heated from 100 to 150 °C under N_2. Similarly, the heat capacity of mmen-Mn_2(dobpdc) was calculated to be 1.5 J/g·K between 70 and 120 °C under N_2.

Supplementary Figures

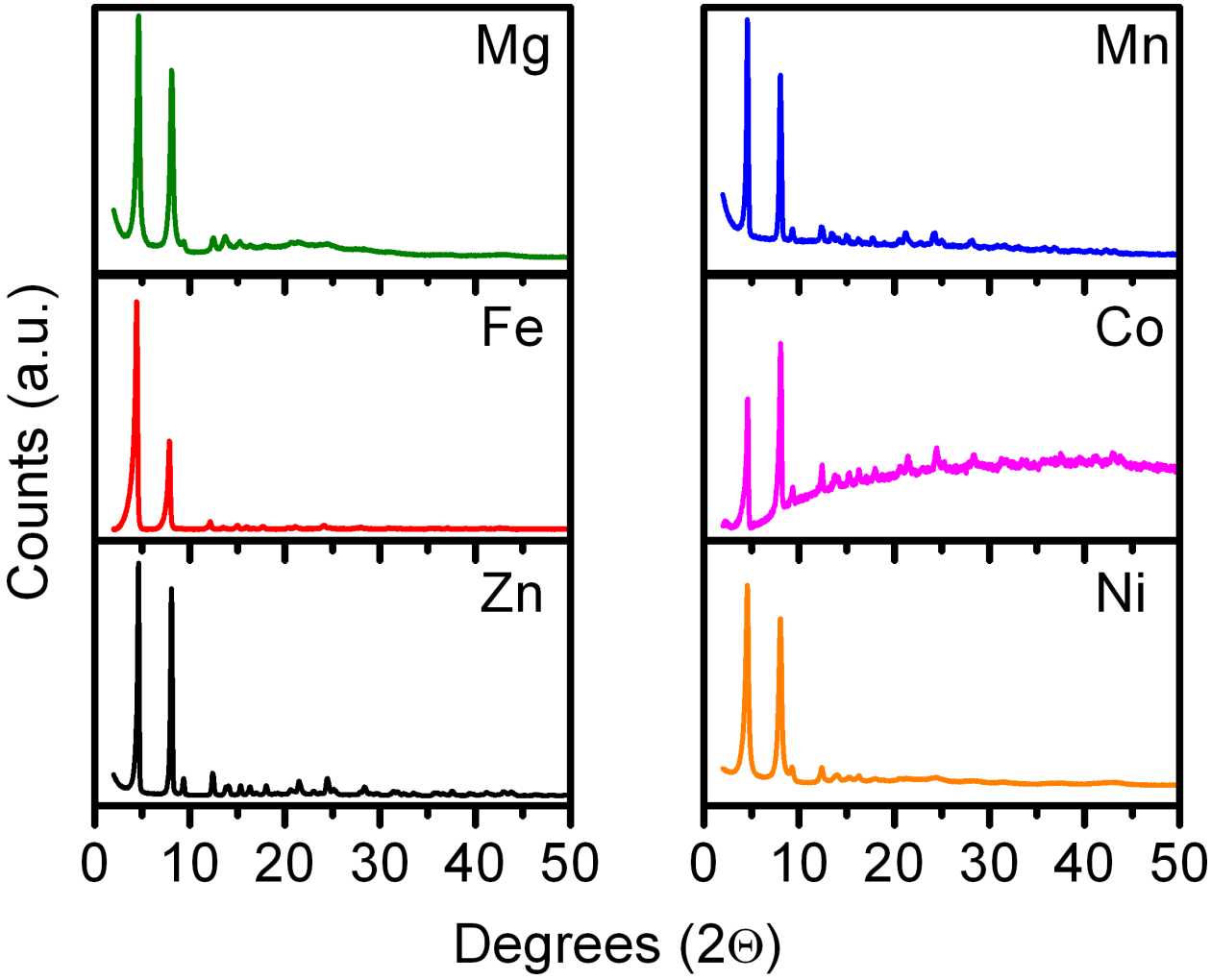

Fig. S1 | Powder X-ray diffraction patterns for Mg_2(dobpdc), Mn_2(dobpdc), Co_2(dobpdc), Fe_2(dobpdc), Zn_2(dobpdc), and Ni_2(dobpdc) at room temperature (λ = 1.5406).

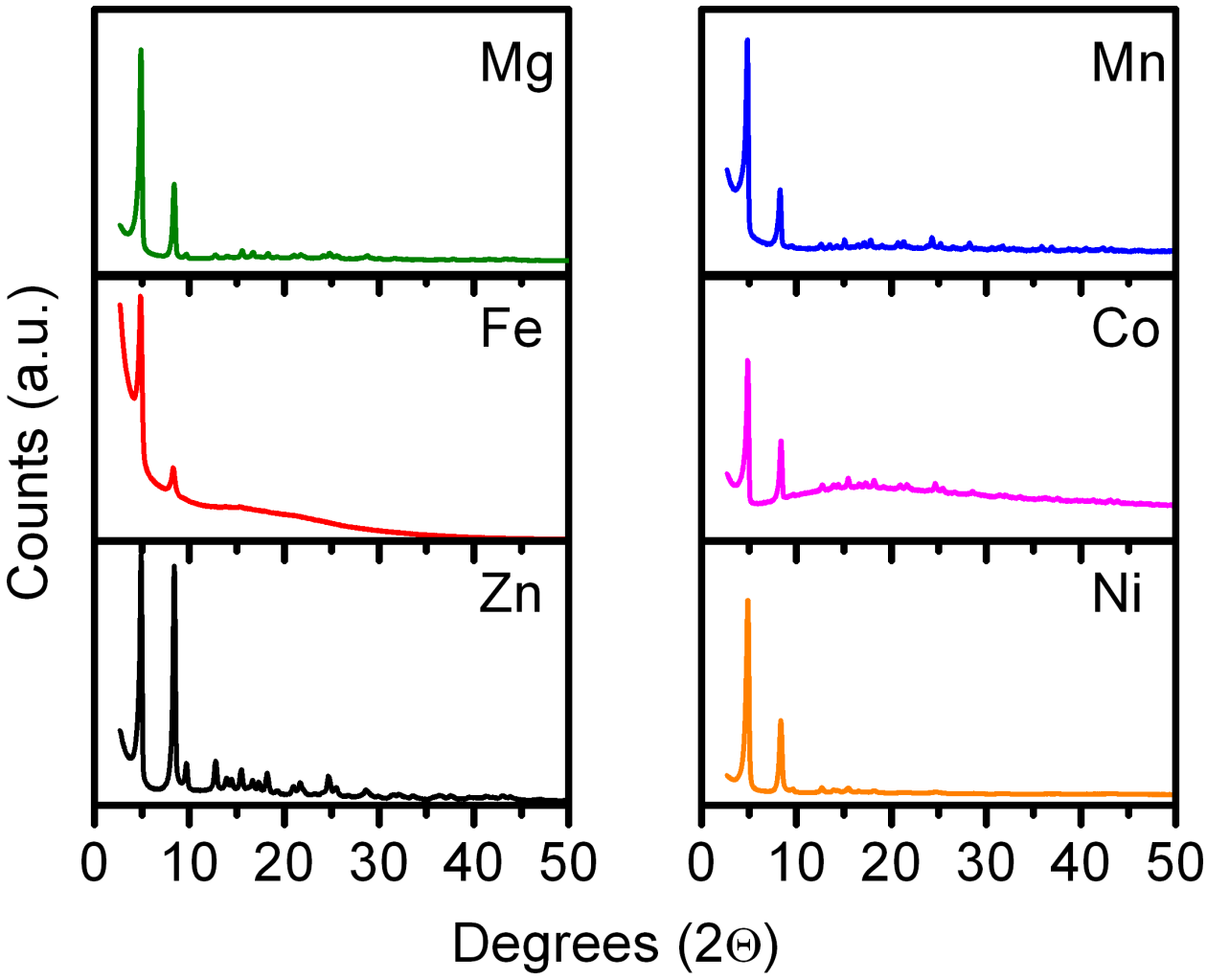

Fig. S2 | Powder X-ray diffraction patterns for mmen-Mg_2(dobpdc), mmen-Mn_2(dobpdc), mmen-Co_2(dobpdc), mmen-Fe_2(dobpdc), mmen-Zn_2(dobpdc), and mmen-Ni_2(dobpdc) at room temperature ($\lambda = 1.5406$).

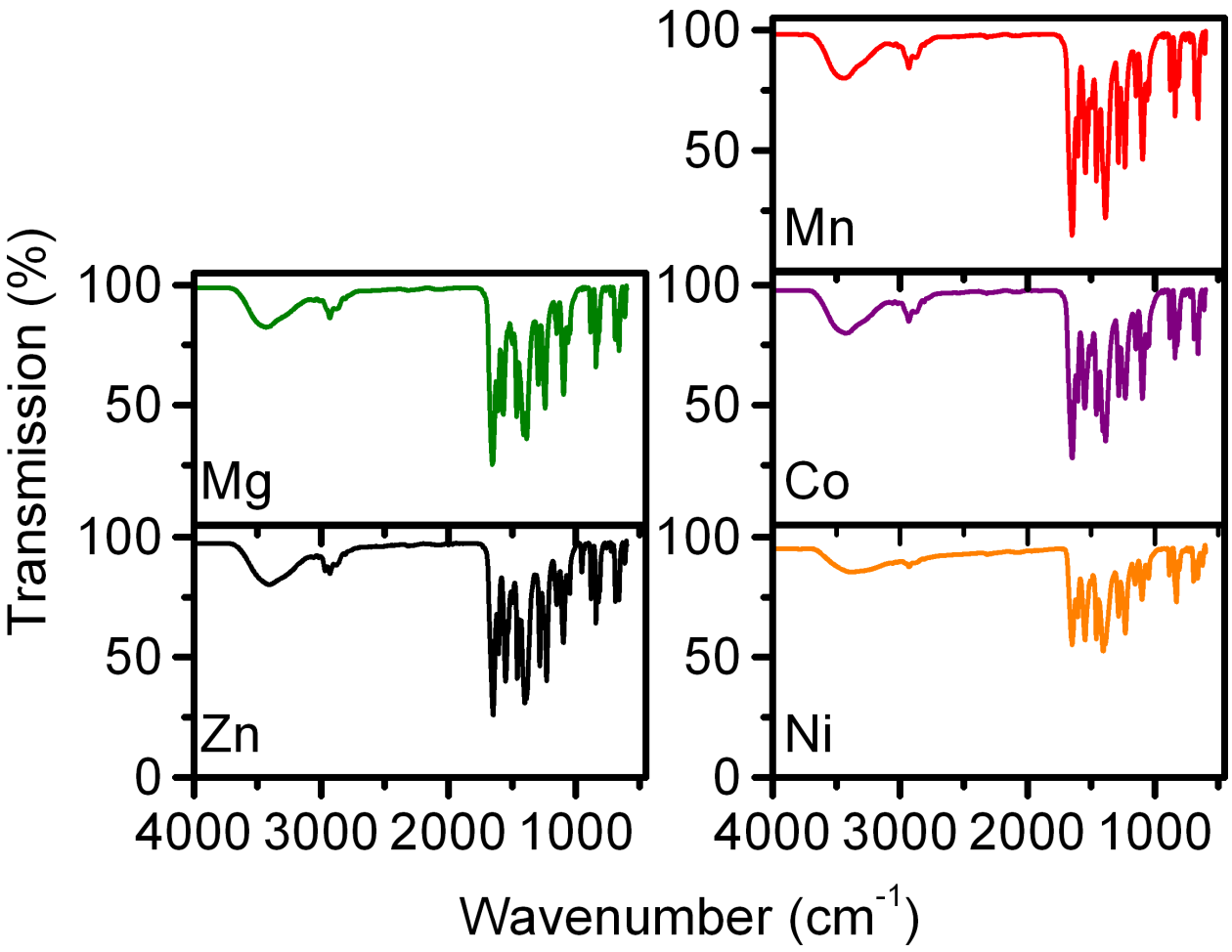

Fig. S3 | Infrared spectra for DMF solvated samples of Mg_2(dobpdc), Mn_2(dobpdc), Co_2(dobpdc), Ni_2(dobpdc), and Zn_2(dobpdc) at room temperature.

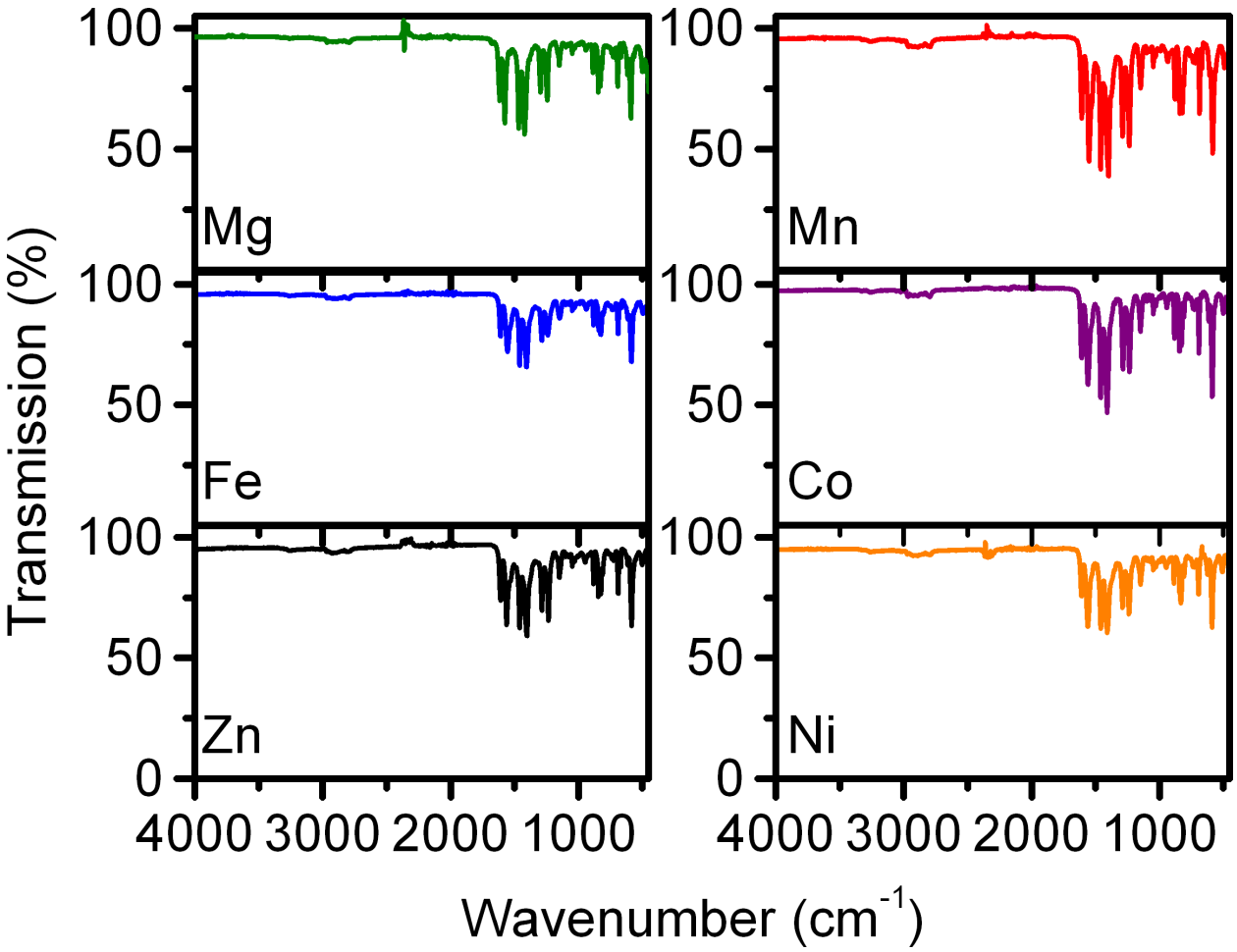

Fig. S4 | Infrared spectra for mmen-Mg_2(dobpdc), mmen-Mn_2(dobpdc), mmen-Co_2(dobpdc), mmen-Fe_2(dobpdc), mmen-Zn_2(dobpdc), and mmen-Ni_2(dobpdc) at room temperature.

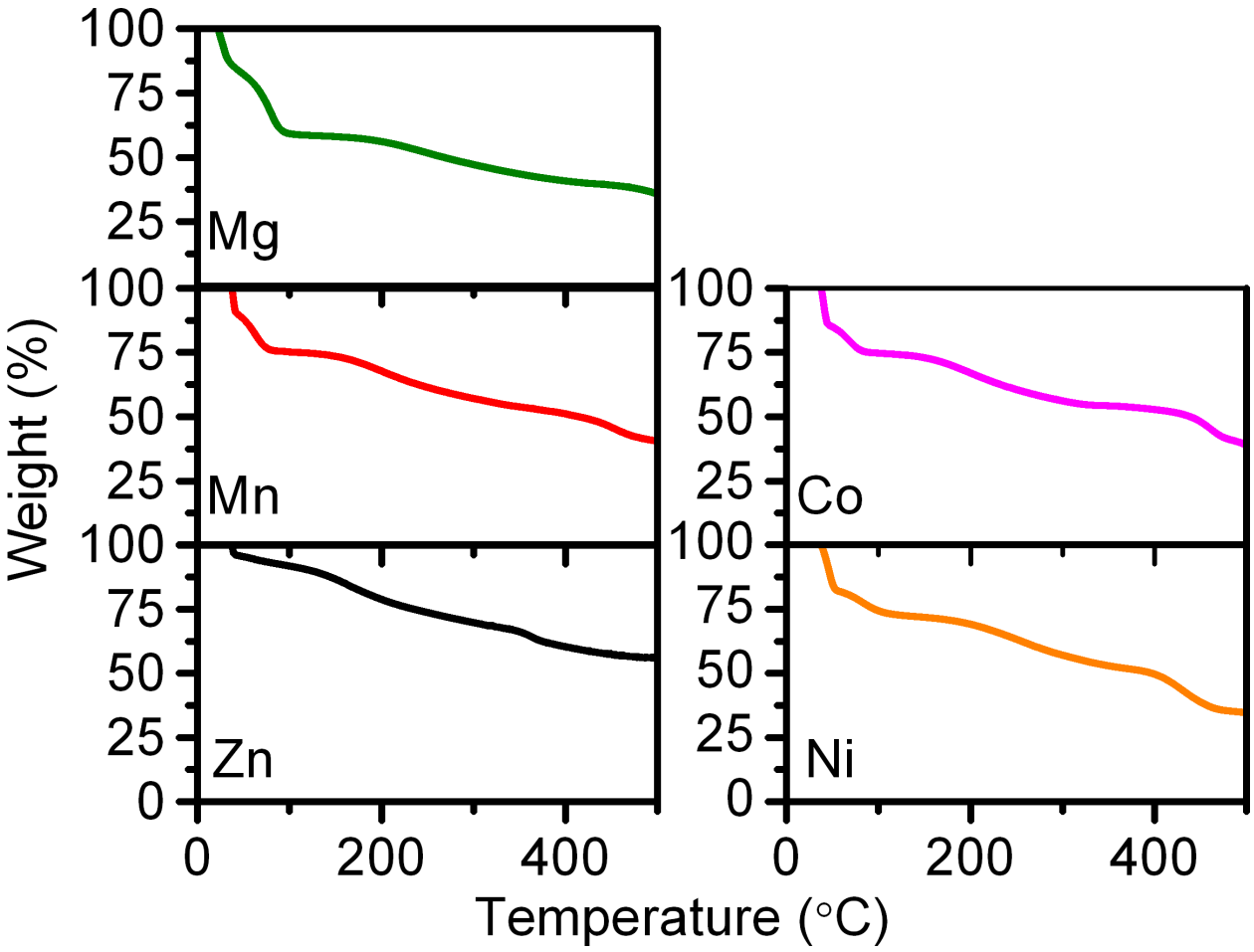

Fig. S5 | Thermogravimetric analysis data for DMF solvated samples of Mg_2(dobpdc), Mn_2(dobpdc), Co_2(dobpdc), Zn_2(dobpdc), and Ni_2(dobpdc).

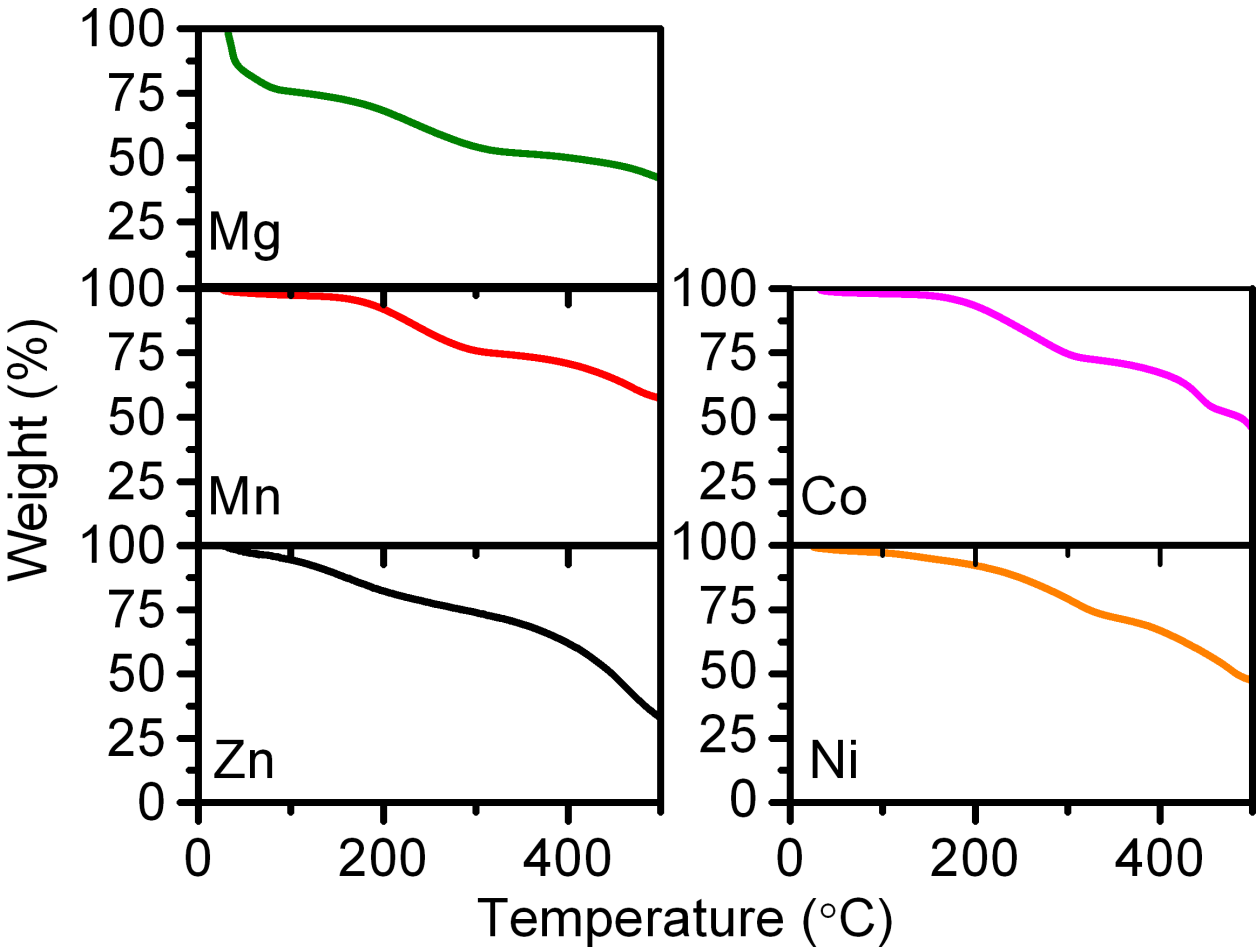

Fig. S6 | Thermogravimetric analysis data of mmen-Mg_2(dobpdc), mmen-Mn_2(dobpdc), mmen-Co_2(dobpdc), mmen-Zn_2(dobpdc), and mmen-Ni_2(dobpdc).

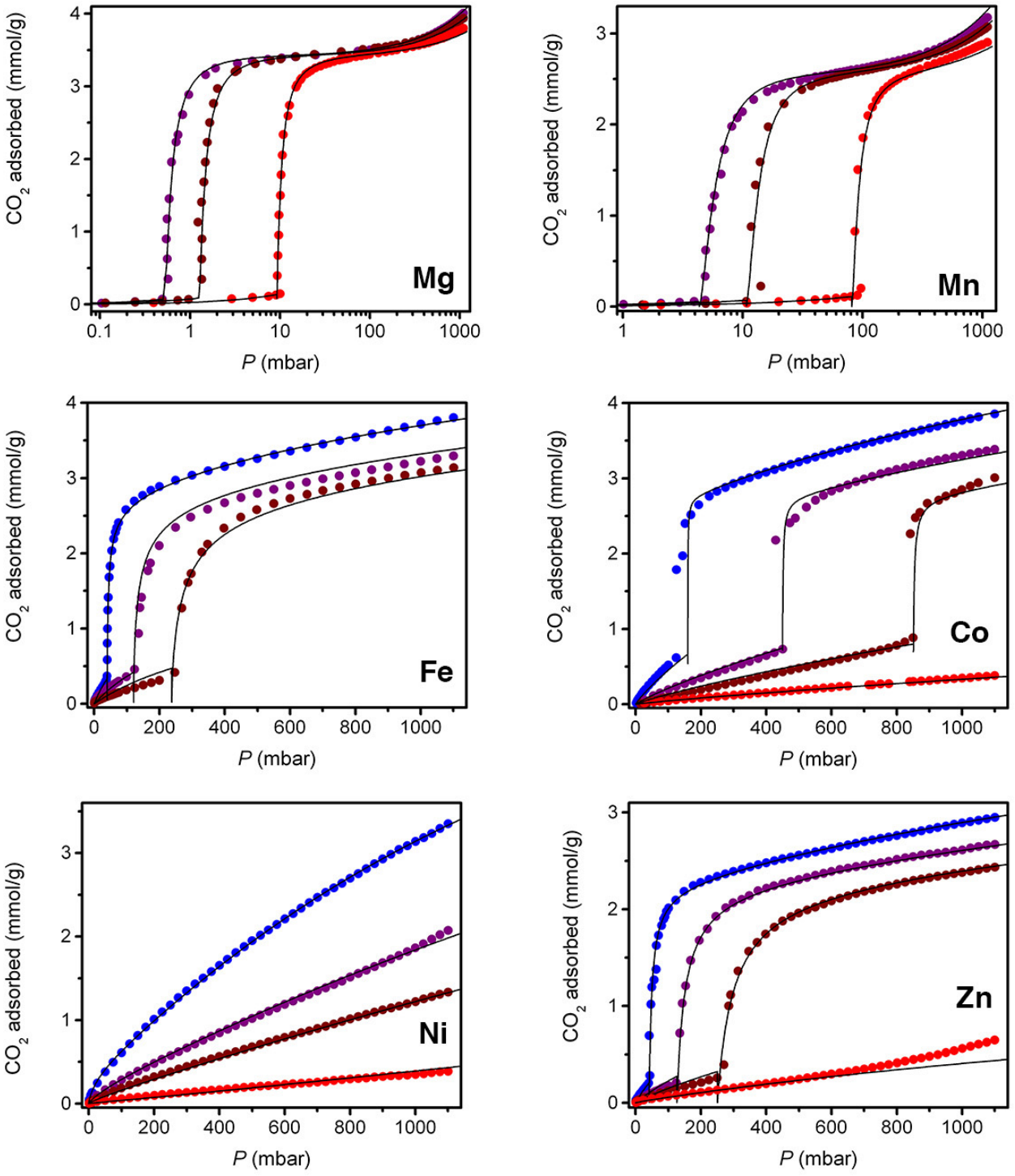

Fig. S7 | Fits to the experimental CO_2 adsorption isotherms (blue: 25 °C; blue-violet: 40 °C; red-violet: 50 °C; red: 75 °C) for the mmen-M_2(dobpdc) series are indicated as black lines.

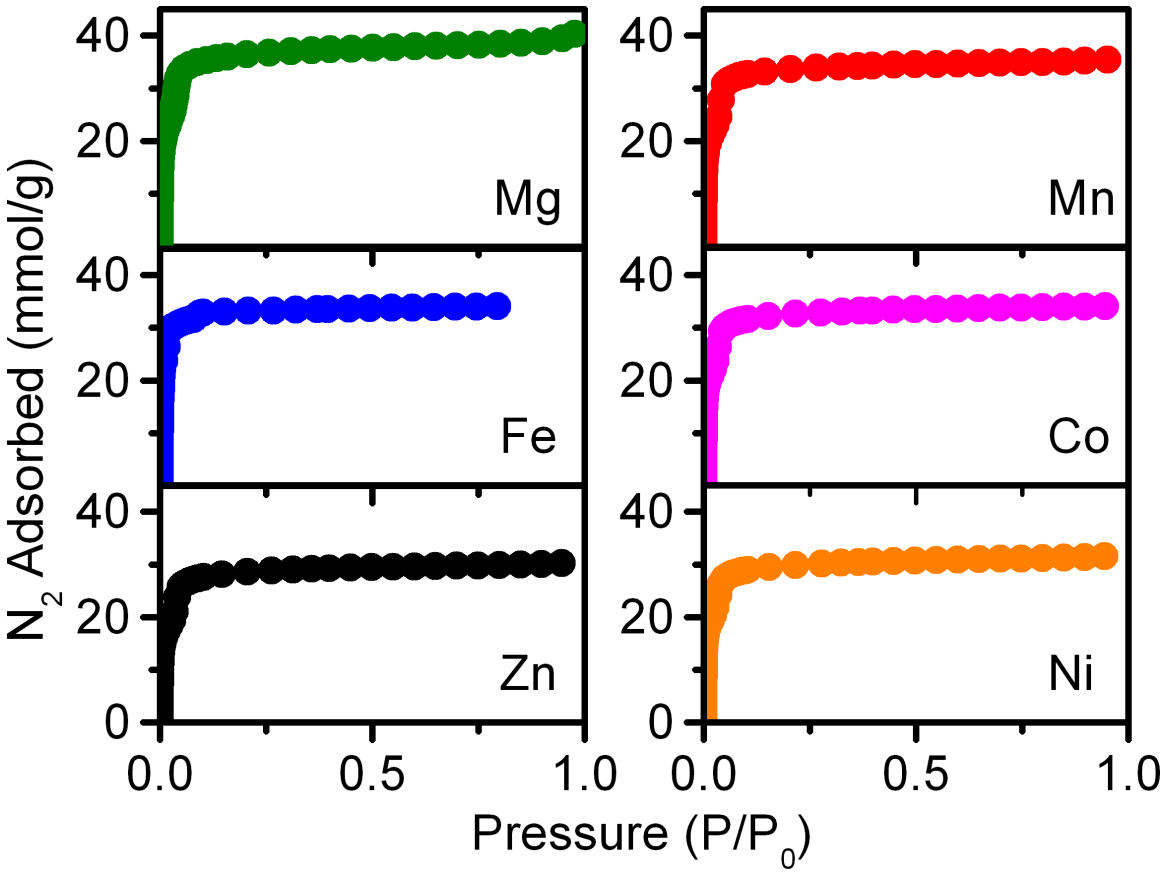

Fig. S8 | Nitrogen adsorption isotherms at 77 K of Mg_2(dobpdc), Mn_2(dobpdc), Fe_2(dobpdc), Co_2(dobpdc), Zn_2(dobpdc), and Ni_2(dobpdc).

Supplementary Tables

Table S1 | Unit cell parameters for mmen-Mn_2(dobpdc) and CO_2-mmen-Mn_2(dobpdc).

	a (Å)	*c* (Å)	*V* (Å^3)	*T* (K)	space group
mmen-Mn_2(dobpdc)	21.7291(7)	7.1279(3)	2914.6(2)	100	$P3_221$
CO_2-mmen-Mn_2(dobpdc)	21.6819(4)	7.0794(1)	2882.2(1)	100	$P3_221$
CO_2-mmen-Mn_2(dobpdc)	21.7427(7)	7.0696(2)	2894.4(2)	295	$P3_221$

Table S2 | Rietveld Refinement of mmen-Mn_2(dobpbdc) dosed with 5 mbar He. Values in parenthesis indicate one standard deviation from the parameter value. Temperature = 100 K, space group $P3_221$, a = 21.7291(7) Å, c = 7.1279(3) Å, V = 2914.6(2) Å^3. Goodness-of-fit parameters: R_{wp} = 5.82%, R_p = 4.52%, χ^2 = 0.907.

atom	*x*	*y*	*z*	*multiplicity*	*occupancy*	U_{iso} (Å^2)
Mn	0.6120(9)	0.2744(9)	1.141(2)	6	1	0.042(5)
O1	0.655(4)	0.241(5)	0.95(1)	6	1	0.075(11)[a]
O2	0.634(3)	0.283(4)	0.62(1)	6	1	0.075(11)[a]
O3	0.586(4)	0.209(3)	0.38(1)	6	1	0.075(11)[a]
C1	0.622(6)	0.175(9)	0.87(2)	6	1	0.075(11)[a]
C2	0.597(6)	0.162(8)	0.67(2)	6	1	0.075(11)[a]
C3	0.565(5)	0.095(7)	0.60(2)	6	1	0.075(11)[a]
C4	0.554(5)	0.035(5)	0.71(2)	6	1	0.075(11)[a]
C5	0.579(5)	0.049(6)	0.90(2)	6	1	0.075(11)[a]
C6	0.613(6)	0.121(7)	0.98(2)	6	1	0.075(11)[a]
C7	0.606(7)	0.221(7)	0.55(2)	6	1	0.075(11)[a]
H1	0.572	0.010	0.98	6	1	0.075(11)[a]
H2	0.629	0.129	1.10	6	1	0.075(11)[a]
H3	0.549	0.088	0.48	6	1	0.075(11)[a]
N1m	0.497(3)	0.208(5)	1.04(1)	6	1.00(5)	0.01(3)
C1ma[b]	0.46(1)	0.25(2)	1.01(6)	6	0.50(15)	0.28(6)[c]
C1mb[b]	0.48(2)	0.20(2)	0.83(7)	6	0.50(15)	0.28(6)[c]
C2m	0.446(96)	0.13(1)	1.04(3)	6	1.00(5)	0.28(6)[c]
C3m	0.396(9)	0.120(8)	1.20(2)	6	1.00(5)	0.28(6)[c]
N2m	0.427(8)	0.118(7)	1.38(2)	6	1.00(5)	0.28(6)[c]
C4m	0.413(9)	0.047(6)	1.43(3)	6	1.00(5)	0.28(6)[c]
H4	0.409	0.216	1.05	6	1.00(5)	0.28(6)[c]
H5	0.479	0.288	1.09	6	1.00(5)	0.28(6)[c]
H6	0.458	0.258	0.88	6	1.00(5)	0.28(6)[c]
H7	0.443	0.200	0.80	6	1.00(5)	0.28(6)[c]
H8	0.525	0.235	0.77	6	1.00(5)	0.28(6)[c]
H9	0.479	0.153	0.80	6	1.00(5)	0.28(6)[c]
H10	0.422	0.116	0.92	6	1.00(5)	0.28(6)[c]
H11	0.472	0.106	1.06	6	1.00(5)	0.28(6)[c]
H12	0.386	0.159	1.20	6	1.00(5)	0.28(6)[c]
H13	0.352	0.076	1.18	6	1.00(5)	0.28(6)[c]
H14	0.467	0.159	1.40	6	1.00(5)	0.28(6)[c]
H15	0.373	0.013	1.35	6	1.00(5)	0.28(6)[c]
H16	0.454	0.043	1.40	6	1.00(5)	0.28(6)[c]
H17	0.401	0.038	1.56	6	1.00(5)	0.28(6)[c]

[a]The thermal parameters for all of atoms of the dobpdc^{4-} ligand were constrained to be equivalent. [b]The CH_3 groups on each Mn-bound N (N1m) are disordered over two positions. [c]With the exception of N1m, the thermal parameters for all atoms of mmen were constrained to be equivalent.

Table S3 | Rietveld Refinement of 100K-CO_2-mmen-Mn_2(dobpbdc), which was dosed with 5 mbar CO_2 at ambient temperature. Values in parenthesis indicate one standard deviation from the parameter value. Temperature = 100 K, space group $P3_221$, a = 21.6819(4) Å, c = 7.0794(1) Å, V = 2882.2(1) Å^3. Goodness-of-fit parameters: wRp = 6.69%, Rp = 5.14%, χ^2 = 1.31.

atom	*x*	*y*	*z*	*multiplicity*	*occupancy*	U_{iso} (Å^2)
Mn	0.6096(3)	0.2717(3)	1.1455(6)	6	1	0.015(1)
O1	0.6595(9)	0.2387(9)	0.959(3)	6	1	0.011(3)[a]
O2	0.644(1)	0.282(1)	0.595(2)	6	1	0.011(3)[a]
O3	0.594(1)	0.2023(9)	0.379(3)	6	1	0.011(3)[a]
C1	0.632(2)	0.180(2)	0.871(4)	6	1	0.011(3)[a]
C2	0.611(2)	0.165(2)	0.681(5)	6	1	0.011(3)[a]
C3	0.576(2)	0.096(2)	0.617(4)	6	1	0.011(3)[a]
C4	0.563(1)	0.039(2)	0.714(4)	6	1	0.011(3)[a]
C5	0.588(1)	0.050(1)	0.897(4)	6	1	0.011(3)[a]
C6	0.613(2)	0.114(1)	0.987(4)	6	1	0.011(3)[a]
C7	0.618(2)	0.219(2)	0.542(4)	6	1	0.011(3)[a]
H1	0.583	0.010	0.965	6	1	0.011(3)[a]
H2	0.626	0.119	0.117	6	1	0.011(3)[a]
H3	0.562	0.085	0.488	6	1	0.011(3)[a]
O1x	0.509(1)	0.196(1)	1.043(3)	6	0.839(8)	0.005(7)
C1x	0.452(2)	0.191(3)	1.059(5)	6	0.839(8)	0.04(1)
O2x	0.425(2)	0.201(2)	1.212(5)	6	0.839(8)	0.09(1)
N1m	0.443(2)	0.227(2)	0.905(5)	6	0.839(8)	0.05(1)
C1m	0.373(2)	0.227(2)	0.863(5)	6	0.839(8)	0.06(2)
C2m	0.457(2)	0.205(3)	0.729(6)	6	0.839(8)	0.07(2)
C3m	0.418(3)	0.129(3)	0.661(8)	6	0.839(8)	0.09(2)
N2m	0.445(4)	0.125(3)	0.47(1)	6	0.839(8)	0.32(5)
C4m	0.400(2)	0.053(2)	0.370(5)	6	0.839(8)	0.001(11)
H4	0.386	0.259	0.758	6	0.839(8)	0.2
H5	0.338	0.180	0.822	6	0.839(8)	0.2
H6	0.353	0.242	0.962	6	0.839(8)	0.2
H7	0.446	0.231	0.633	6	0.839(8)	0.2
H8	0.507	0.219	0.722	6	0.839(8)	0.2
H9	0.428	0.100	0.748	6	0.839(8)	0.2
H10	0.368	0.112	0.657	6	0.839(8)	0.2
H11	0.433	0.149	0.387	6	0.839(8)	0.2
H12	0.491	0.145	0.470	6	0.839(8)	0.2
H13	0.370	0.057	0.278	6	0.839(8)	0.2
H14	0.432	0.040	0.310	6	0.839(8)	0.2
H15	0.372	0.018	0.463	6	0.839(8)	0.2

[a]The thermal parameters for all of atoms of the dobpdc^{4-} ligand were constrained to be equivalent.

Table S4 | Rietveld Refinement of 295K-CO2-mmen-Mn_2(dobpdc), which was dosed with 100 mbar CO_2 at ambient temperature. Values in parenthesis indicate one standard deviation from the parameter value. Temperature = 295 K, space group *P*3221, *a* = 21.7427(7) Å, *c* = 7.0696(2) Å, *V* = 2894.4(2) Å3. Goodness-of-fit parameters: wRp = 5.92%, Rp = 4.44%, χ^2 = 1.03.

atom	*x*	*y*	*z*	*multiplicity*	*occupancy*	U_{iso} (Å^2)
Mn	0.6096(8)	0.2717(7)	1.145(2)	6	1	0.036(4)
O1	0.659(3)	0.239(3)	0.959(8)	6	1	0.020(8)[a]
O2	0.644(2)	0.282(3)	0.595(6)	6	1	0.020(8)[a]
O3	0.594(3)	0.202(2)	0.379(7)	6	1	0.020(8)[a]
C1	0.632(4)	0.180(5)	0.87(2)	6	1	0.020(8)[a]
C2	0.611(4)	0.165(6)	0.68(1)	6	1	0.020(8)[a]
C3	0.576(4)	0.096(5)	0.62(1)	6	1	0.020(8)[a]
C4	0.563(4)	0.039(4)	0.71(1)	6	1	0.020(8)[a]
C5	0.588(4)	0.050(4)	0.90(1)	6	1	0.020(8)[a]
C6	0.613(4)	0.114(5)	0.99(1)	6	1	0.020(8)[a]
C7	0.618(5)	0.219(5)	0.54(1)	6	1	0.020(8)[a]
H1	0.583	0.097	0.965	6	1	0.020(8)[a]
H2	0.626	0.119	0.117	6	1	0.020(8)[a]
H3	0.562	0.085	0.488	6	1	0.020(8)[a]
O1x	0.509(4)	0.196(3)	1.04(1)	6	0.90(2)	0.07(4)
C1x	0.452(8)	0.191(9)	1.06(1)	6	0.90(2)	0.15(2)[b]
O2x	0.425(5)	0.201(5)	1.21(2)	6	0.90(2)	0.15(2)[b]
N1m	0.443(6)	0.227(6)	0.91(2)	6	0.90(2)	0.15(2)[b]
C1m	0.373(7)	0.227(6)	0.86(2)	6	0.90(2)	0.15(2)[b]
C2m	0.457(6)	0.205(8)	0.73(2)	6	0.90(2)	0.15(2)[b]
C3m	0.418(8)	0.129(8)	0.66(2)	6	0.90(2)	0.15(2)[b]
N2m	0.445(5)	0.125(6)	0.47(2)	6	0.90(2)	0.15(2)[b]
C4m	0.400(7)	0.053(5)	0.37(2)	6	0.90(2)	0.15(2)[b]
H4	0.386	0.259	0.758	6	0.90(2)	0.19
H5	0.338	0.180	0.822	6	0.90(2)	0.19
H6	0.353	0.242	0.962	6	0.90(2)	0.19
H7	0.446	0.231	0.633	6	0.90(2)	0.19
H8	0.507	0.219	0.722	6	0.90(2)	0.19
H9	0.428	0.100	0.748	6	0.90(2)	0.19
H10	0.368	0.112	0.657	6	0.90(2)	0.19
H11	0.433	0.149	0.387	6	0.90(2)	0.19
H12	0.491	0.145	0.470	6	0.90(2)	0.19
H13	0.370	0.057	0.278	6	0.90(2)	0.19
H14	0.432	0.040	0.310	6	0.90(2)	0.19
H15	0.372	0.018	0.463	6	0.90(2)	0.19

[a]The thermal parameters for all of atoms of the dobpdc^{4-} ligand were constrained to be equivalent. [b]With the exception of O1x, the thermal parameters for all atoms of mmen were constrained to be equivalent.

Table S5 | Calculated BET surface areas from 77 K N_2 adsorption measurements and their fit parameters for the six M_2(dobpdc) metal-organic frameworks prior to amine functionalization are reported here. Owing to the movement of the diamine appended to the pore surfaces, BET surfaces of the amine-functionalized frameworks were not found to accurately measure their porosity.

metal	*BET* (m^2/g)	*slope*	*y-int.*	P_{low}	P_{high}	q_{sat}	*C*
Mg	3326	2.919E-02	1.383E-04	1.401E-03	2.189E-03	34.10	212.0
Mn	3019	3.220E-02	9.659E-05	1.723E-03	2.239E-03	30.96	334.4
Fe	2892	3.371E-02	1.539E-05	9.612E-04	1.808E-03	29.65	219.1
Co	2928	3.321E-02	9.245E-05	1.515E-03	2.278E-03	30.02	360.3
Ni	2719	3.572E-02	1.448E-04	1.617E-03	2.537E-03	27.88	247.6
Zn	2520	3.860E-02	1.009E-04	2.002E-03	2.962E-03	25.84	383.5

Table S6 | Summary of piecewise Lagnmuir-Freundlich fit parameters for stepped CO_2 isotherms of mmen-M_2(dobdc).

	Mg	Mn	Co	Fe	Zn
n_{sat1} (mmol g^{-1})	8.1	1.0	8.2	1.4	2.2
S_1 (R)	–13.9	–9.8	–17.2	–15.0	–14.7
H_1 (kJ/mol)	–38.6	–26.6	–40.7	–42.2	–38.4
v_1	0.7	0.6	0.9	1.0	0.9
n_{sat2a} (mmol g^{-1})	3.4	2.5	2.7	2.5	2.2
S_{2a} (R)	–17.5	–20.0	–14.3	–18.6	–18.3
H_{step} (kJ/mol)	–74.1	–75.9	–53.5	–56.9	–57.3
v_{2a}	1.2	1.4	0.9	0.7	1.0
n_{sat2b} (mmol g^{-1})	12.0	15.0	4.9	9.6	3.5
S_{2b} (R)	10.0	11.7	10.1	7.9	10.1
H_{2b} (kJ/mol)	18.3	22.4	22.2	14.7	21.8
v_3	0.8	0.9	0.9	0.6	0.9
$P_{step,T0}$	0.5	4.3	450.0	120.8	127.0
T_0	313.15	313.15	313.15	313.15	313.15

Table S7 | Summary of dual-site Langmuir-Freundlich fit parameters for CO_2 isotherms of mmen–Ni_2(dobdc).

	Ni
n_{sat1a} (mmol g^{-1})	6.6
S_{1a} (R)	–18.7
H_{1a} (kJ/mol)	–45.1
v_{1a}	1.2
n_{sat2b} (mmol g^{-1})	0.7
S_{2b} (R)	–25.3
H_{2b} (kJ/mol)	–68.2
v_{2b}	0.8